A Multi-State Notch Filter for GNSS Jamming Mitigation

Daniele Borio

EC Joint Research Centre, Institute for the Protection and Security of the Citizen, Ispra, Italy
Email: daniele.borio@ieee.org

***Abstract*—Adaptive notch filters have been proven to be effective solutions for mitigating the impact of jamming and extending the operational capabilities of GNSS receivers.**
In this paper, a multi-state model is at first proposed for the characterization of jamming signals. In particular, jamming signals can move outside the input band of the victim receiver and their instantaneous frequency can be affected by abrupt jumps. These features are accounted for in the multi-state model which is used to design a new class of adaptive notch filters able to cope with the state transitions of the jamming signal.
The adaptive notch filter proposed has been designed to be computationally efficient and to track the fast frequency variations of a jamming signal. The performance of the technique proposed is experimentally studied using a real cigarette lighter jammer and a custom software receiver. The tests show the benefits of the notch filter proposed.

***Index Terms*—Galileo, GNSS, GPS, Interference Cancellation, Jamming, Notch Filter, State Model**

I. Introduction

The modernization of the Global Positioning System (GPS) and the development of new Global Navigation Satellite Systems (GNSSs), such as Galileo, GLONASS and Beidou, are fostering the development of new location-based applications. GPS boxes can be used by insurance companies to monitor the behavior of a driver and to adjust the insurance premium accordingly. Freight companies can use GPS to track the position of their fleet. This type of application inevitably requires the monitoring of the user behavior and introduces privacy issues. This motivates the adoption of GNSS jammers which are small, portable devices able to broadcast powerful signals in the GNSS bands disrupting the operations of GNSS receivers.

Several countermeasures can be adopted at the receiver level to mitigate the impact of GNSS jammers [1], [2]. In particular, adaptive notch filters have been proven to be an effective solution for mitigating the impact of jamming and extending the operational capabilities of GNSS receivers. In [1], an adaptive notch filter, originally conceived for the removal of Continuous Wave Interference (CWI), was tested in the presence of a jamming signal. [2] suggested a Kalman filter for tracking the fast variations of the instantaneous frequency of the jamming signal. Despite the encouraging results obtained by [1] and [2], the approaches proposed are effective only when the instantaneous frequency of the jamming signal varies in a continuous manner. Jammer signals can however move outside the input band of the receiver front-end and their instantaneous frequency can be affected by abrupt jumps [3], [4]. The algorithms suggested in [1] and [2] are unable to effectively cope with these phenomena.

In this paper, a multi-state model is proposed for the characterization of jamming signals. The model captures the signal features mentioned above and it is used for the design of a new strategy for tracking the fast frequency variations of jamming signals. The technique proposed is integrated in a constrained single pole notch filter [5], [6] which is adopted to remove the jamming signal.

The notch filter is at first analyzed using the Interference Cancellation (IC) principle which is effectively implemented by the notch filter. This fact is exploited and the multi-state model is used for the adaptation of the filter zero. In particular, a different adaptation strategy is adopted depending on the state of the jamming signal.

The adaptive notch filter proposed has been designed to be computationally efficient and to track the fast frequency variations of a jamming signal. The performance of the technique proposed is experimentally studied using a cigarette lighter jammer and a custom software receiver. In particular, the base-band data collected according to the experimental setup described in [1] were used to test the performance of the algorithm proposed. The tests performed show the advantage of the multi-state notch filter which extends the operational capabilities of GNSS receivers.

The remainder of this paper is organized as follows. In Section II, the IC principle is reviewed and the constrained single pole notch filter is introduced as a form of IC for single component signals. The multi-state jamming model is discussed in Section III and the multi-state notch filter is described in Section IV. The filter performance is evaluated in Section V and, finally, conclusions are drawn in Section VI.

II. The Interference Cancellation Principle

The signal at the input of an adaptive notch filter can be modeled as

$$y[n] = x[n] + i[n] + \eta[n] \tag{1}$$

where

- $x[n]$ is the useful signal containing the different GNSS components which will be used for receiver operations

- $i[n]$ is an interference source
- $\eta[n]$ is a noise term usually modeled as a complex circularly symmetric Gaussian random process. The samples of $\eta[n]$ are independent and identically distributed (i.i.d).

Sequence $y[n]$ has been obtained by filtering, down-converting and digitizing an analog signal, $y(t)$, with a sampling interval, T_s. $f_s = \frac{1}{T_s}$ is the sampling frequency and n is the time index used to denote uniform time sampling.
When IC is adopted, the interfering signal is at first removed from $y[n]$ and processing is applied to

$$\tilde{y}[n] = y[n] - i[n]. \tag{2}$$

Since $i[n]$ is usually not known, an estimation technique is required to reconstruct it and to obtain $\hat{i}[n]$. $i[n]$ is usually estimated by considering a specific signal model which depends only on a reduced number of parameters. Consider for example, a single component signal [7]

$$i[n] = A[n] \exp\{j\phi[n]\} \tag{3}$$

where $A[n]$ and $\phi[n]$ are two real signals with

$$A[n] \in [0, +\infty) \quad \text{and} \quad \phi[n] \in (-\pi, \pi]. \tag{4}$$

Although (3) is quite general, the hypothesis assumed by the single component model is that $i[n]$ is instantaneously narrow band [7], i.e., it has a single frequency component at each instant in time. The instantaneous frequency of a single component signal is defined as the discrete derivative of its phase:

$$f_i[n] = \frac{1}{2\pi} \left(\phi[n] - \phi[n-1]\right). \tag{5}$$

Note that even if signal model (3) is composed of a single complex exponential, fast phase variations may lead to a wideband signal. Model (3) is opposed to the multi-component signal

$$i[n] = \sum_{l}^{L-1} A_l[n] \exp\{j\phi_l[n]\}. \tag{6}$$

Single component signals can be generated by a first order recurrence equation

$$i[n] = a[n]i[n-1] \tag{7}$$

where $a[n]$ is a time-varying coefficient. From (3),

$$\begin{aligned} a[n] = \frac{i[n]}{i[n-1]} &= \frac{A[n]}{A[n-1]} \exp\{j\left(\phi[n] - \phi[n-1]\right)\} \\ &= \frac{A[n]}{A[n-1]} \exp\{j2\pi f_i[n]\}. \end{aligned} \tag{8}$$

Continuous Wave (CW) and chirp signals are single component [8]. The single component assumption and recurrence equation (7) allow the prediction of $i[n]$ from the past sample, $i[n-1]$. This principle is exploited in a single pole notch filter which is characterized by the following transfer function:

$$H_n(z) = \frac{1 - z_0[n]z^{-1}}{1 - k_a z_0[n] z^{-1}} \tag{9}$$

where $z_0[n]$ is the complex zero of the filter and k_a is the pole contraction factor. In particular, the output of the Moving Average (MA) part of the filter is obtained as

$$\begin{aligned} y_{MA}[n] = y[n] - z_0[n]y[n-1] &= x[n] - z_0[n]x[n-1] \\ &+ (i[n] - z_0[n]i[n-1]) + \eta[n] - z_0[n]\eta[n-1]. \end{aligned} \tag{10}$$

Ideally, the role of the MA part of the filter is to remove the interference source, i.e. to perform IC exploiting (2) and (7). Thus, $z_0[n]$ should be adapted in order to satisfy

$$z_0[n] = \frac{i[n]}{i[n-1]} = a[n]. \tag{11}$$

The Auto Regressive (AR) part of (9) is used to minimize the impact of the MA part of the filter on the useful signal component. Distortions on the useful signal are reduced as k_a approaches 1. Specific constraints can be used to simplify the estimation of $a[n]$. For example, if $i[n]$ has an amplitude which is slowly varying with time, it is possible to constrain $z_0[n]$ to lay on the unit circle:

$$|z_0[n]| = 1 \tag{12}$$

and update only the estimate of the signal instantaneous frequency.
In the following, a simple adaptation criterion is developed considering constraint (12). Note that (8) assumes that $A[n-1] \neq 0$. However, as discussed in Section III, the jamming signal may not be present or exit the receiver band. For this reason, a multi-state approach is adopted to deal with the signal absence.

III. Multi-State Jamming Signal Model

Several papers [3], [4], [9] considered the problem of characterizing the signals transmitted by GNSS jammers. The characterization was however in terms of transmitted power, frequency range and sweep time: [3] provided an initial analysis showing that although most of the jamming signals are linearly frequency modulated, deviations from a linear frequency trend can occur. [9] extended the analysis considering the mechanisms used for the signal generation. Finally, [4] combined new experimental results with the findings from [3] and [9] to provide a more complete characterization of jamming signals. Although these results provide a qualitative and quantitative description of jamming signals, a functional state model of the received jamming signal is required for the design of effective mitigation techniques. A mitigation algorithm should adopt a different behaviour depending on the state of the jamming signal.
In particular, from the results presented in [3], [9] and [4], the three-state model depicted in Fig. 1 can be derived. The jamming signals can be

- in a *Continuous Frequency Variation (CFV) state*: the instantaneous frequency of the jamming signal is varying in a continuous manner, for example in a linear way. The signal is not affected by frequency jumps.

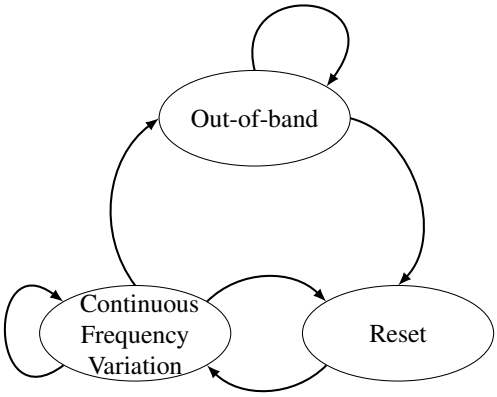

Fig. 1. State model for the signal transmitted by a GNSS jammer.

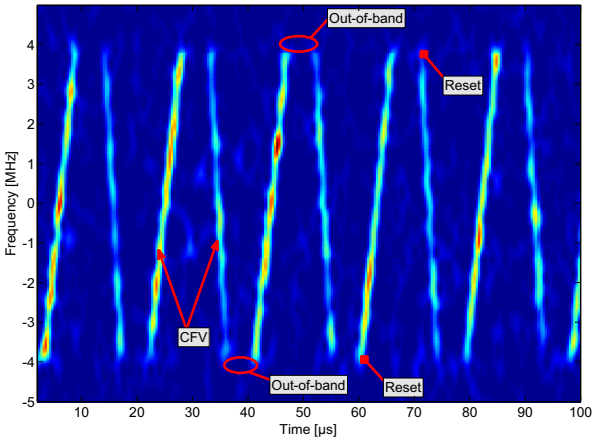

Fig. 2. Time-frequency evolution of a simulated jamming signal. The signal enters the different states described by the model in Fig. 1.

- *Out-of-band*: the jamming signal is outside the band of the victim GNSS receiver and thus it is filtered out.
- *Reset*: the jammer is affected by a reset and the jamming signal is affected by a frequency jump. A reset is a transitory state and may also occur when the jamming signal move from the out-of-band to the CFV condition.

Possible transitions between the different states are also indicated in Fig. 1. The model in Fig. 1 is general and can be used to describe most of the jamming signals analysed in the literature. Note that, depending on the jamming signal considered, some of the states may be missing. For example, in [2] only jamming signals not affected by a frequency reset were analysed and the Kalman filter developed cannot cope with this type of phenomenon. In order to illustrate the state model developed, the time-frequency evolution of a simulated jamming signal is analyzed in Fig. 2. The signal has been generated in order to mimic the characteristics of the real jammer considered in [2] (Fig. 8). The different signal states are clearly indicated. When the jammer transits from the out-of-band to CFV state, a reset occurs.

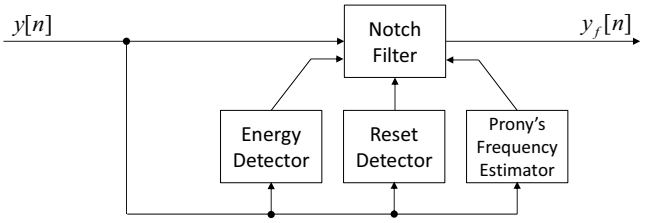

Fig. 3. Structure of the adaptive notch filter designed to cope with a time-varying jamming signal.

IV. Multi-State Notch Filter

The structure of the adaptive notch filter developed to cope with a time-varying jamming signal is shown in Fig. 3. In particular, three functional blocks have been introduced to determine the state of the jamming signal and eventually estimate its instantaneous frequency. The first block aims at determining if the jamming signal is present. As detailed in Section IV-A, a simple energy detector has been selected for its low computational complexity. The energy detector has to be able to cope with potentially rapid changes between the CFV to the out-of-band states.
The second block in Fig. 3 has been introduced to determine if a reset occurred. Finally, Prony's frequency estimator [10] has been selected to estimate the instantaneous frequency of the jamming signal and track its variations. Note that different algorithms could have been selected to implement the three functional blocks described above. In this work, computational efficiency was considered a major driver with respect to estimation and detection performance. Thus, computationally efficient techniques able to effectively operate in the presence of strong jamming signals have been selected.

A. Energy Detector

In order to verify that the jamming signal is indeed inside the receiver band, a simple energy detector [11] has been adopted. In particular, the energy at the time instant n is computed as

$$E[n] = \frac{1}{L}\sum_{i=0}^{L-1} |y[n-i]|^2 \tag{13}$$

where L defines the number of samples used to estimate the signal energy. $E[n]$ is compared against a decision threshold and the jamming signal is declared present if $E[n]$ passes such threshold. The threshold is set assuming a predefined probability of false alarm, i.e. the probability of erroneously declaring the jamming signal present. In the absence of jamming, $E[n]$ is a scaled central chi-squared random variable with $2L$ degrees of freedom [11]. Thus, the decision threshold can be set exploiting the properties of chi-squared random variables. It is noted that the decision threshold depends on the variance of the noise in (1). This variance can be determined using a noise floor estimator in the absence of interference.
When the jamming signal is declared absent, $z_0[n]$ is set to

zero. In this way, the notch filter defined by (9) becomes an all-pass filter and

$$y_f[n] = y[n] \tag{14}$$

where $y_f[n]$ is the signal at the filter output.
When the jamming signal is detected for the first time, i.e. after a series of epochs of absence, a reset event is declared and the filter initialization described in Section IV-B is performed.

B. Reset Detection

A reset can be detected adopting a small analysis window of size L. This implies that for each processing epoch, the last L input samples are considered. We can assume that L is sufficiently small such that

- only a single reset may occur
- the frequency evolution of the jamming signal can be effectively modeled as linear.

It is also assumed that the jamming signal does not exit of the front-end band. This event is handled by the energy detector described in Section IV-A. If the jammer is declared out-of-band then the reset detector is disabled.
Using these assumptions, the reset detection problem can be formulated as the decision between the two hypotheses

$$H_0: \quad y[k] = A\exp\left\{j(\varphi_0 + 2\pi f_0 kT_s + \pi a_0 k^2 T_s^2)\right\} + \eta[k] \quad \forall k = n, n-1, ..., n-L+1 \tag{15}$$

$$H_1: \quad y[k] = A\exp\left\{j\varphi[k]\right\} + \eta[k] \quad \exists\ k : \varphi[k] \neq \varphi_0 + 2\pi f_0 kT_s + \pi a_0 k^2 T_s^2 \tag{16}$$

where the impact of $x[n]$ in (1) has been neglected. Under the null hypothesis, H_0, all the signal samples are characterized by a linearly modulated frequency and a reset does not occur. The alternative hypothesis, H_1, is linked to the occurrence of a reset and implies that there exists at least one sample which does not follow a linear frequency evolution.
The design of a reset detector can be obtained following the Generalized Likelihood Ratio Test (GLRT) [11] approach. In particular, it is possible to show that a reset detector has to implement the following steps

- at first estimate the frequency and frequency rate terms, f_0 and a_0. This can be done for example using the Maximum Likelihood (ML) approach.
- use the frequency and frequency rate estimates, $\hat{f}_0$ and $\hat{a}_0$ to produce the corrected samples

$$y_c[n] = y[n]\exp\left\{-j\left(2\pi\hat{f}_0 nT_s + \pi\hat{a}_0 n^2 T_s^2\right)\right\}. \tag{17}$$

  Under H_0, all the corrected samples have the same phase, φ_0.
- determine if all the corrected samples have the same phase, for example using the Phase-only ANalysis Of VAriance (PANOVA) approach [12].

The ML estimator for the frequency and frequency rate terms is computationally demanding and requires an exhaustive search on the space defined by these two parameters. For this reason, the following simplified approach has been adopted. The corrected samples

$$\bar{y}_c[n] = y[n]\text{csign}\left(y^*[n-1]\right) \tag{18}$$

are at first computed where the symbol 'csign$(\cdot)$' denotes the complex sign:

$$\text{csign}\left(x\right) = \frac{x}{|x|}. \tag{19}$$

Note the operation in (19) is equivalent to a phase differentiation on the input samples. In this way, input samples following model (15) lead to corrected samples with phase

$$\angle\bar{y}_c[n] = 2\pi\left(f_0 T_s + \frac{1}{2}a_0(2k-1)T_s\right). \tag{20}$$

When small analysis windows are considered and for most of the jammers found in the literature [4], it is possible to show that, for $k = n, n-1, ..., n-L+1$, the following approximation holds

$$2\pi\left(f_0 T_s + \frac{1}{2}a_0(2k-1)T_s\right) \approx 2\pi\left(f_0 T_s + \frac{1}{2}a_0(2n-L)T_s\right) \tag{21}$$

which implies that under H_0, the corrected samples have an almost constant phase. It is noted that a second phase differentiation would have removed the frequency rate term in (20). However, the multiplication in (18) significantly amplifies the impact of the input noise, $\eta[n]$. Moreover, it has been empirically verified that a single phase differentiation leads to the best reset detection capabilities.
The corrected samples are finally used to compute the PANOVA [12] decision variable which is used for reset detection:

$$P[n] = \sum_{i=0}^{L-1}|\bar{y}_c[n-i]| - \left|\sum_{i=0}^{L-1}\bar{y}_c[n-i]\right|. \tag{22}$$

It is noted that in [12], the samples in the summations in (22) are weighted by their relative amplitudes which are assumed to be known. In this case, all the samples have the same amplitude and the weighting is no longer required.
The decision variable, $P[n]$, is compared against a decision threshold and a reset is declared if $P[n]$ passes such threshold. It is noted that the operation in (20) changes the statistical properties of the input samples, $y[n]$, and the corrected samples, $\bar{y}_c[n]$, are no longer affected by Gaussian noise. Thus, the results presented in [12] for setting the decision threshold are no longer valid. A statistical characterization of $P[n]$ is beyond the scope of this paper and it is left for future work. In this case, the decision threshold was empirically determined.
When a jamming signal reset is detected, the notch filter states are also reset and the output signal is set to zero. In particular, after a reset it is not possible to use the input past samples to estimate the signal frequency and thus is not possible to remove interference through filtering. For this reason, signal blanking is adopted and $y_f[n]$ is set to zero.

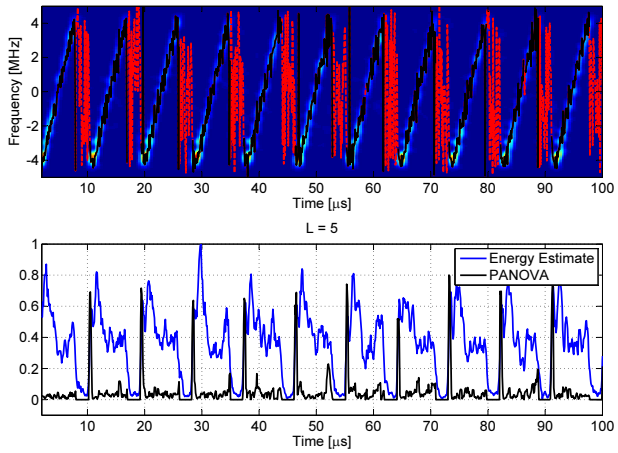

Fig. 4. Illustration of the behavior of the multi-state notch filter when operating on a signal broadcast by a cigarette lighter jammer. In the bottom part, the different metrics have been normalized with respect to their maximum value.

C. Continuous Frequency Variations

When the centre frequency of the jamming signal varies in a continuous way, it can be estimated using several techniques, including a Frequency Lock Loop (FLL) or the stochastic gradient approach used in [13]. In this work, Prony's frequency estimator has been selected and the interference frequency, $f_i[n]$, as been estimated as

$$\hat{f}_i[n] = \frac{1}{2\pi}\angle y[n]y^*[n-1] = \frac{1}{2\pi}\angle \bar{y}_c[n]. \quad (23)$$

Note that frequency estimates can be improved by introducing time averaging

$$\hat{f}_i[n] = \frac{1}{2\pi}\angle \sum_{i=0}^{L-1} \bar{y}_c[n-i] \quad (24)$$

where L is the number of integrations. When dealing with strong jamming signals, i.e. the most critical case for GNSS receivers, a single corrected sample is sufficient to provide good results. Moreover, the use of a single corrected sample guarantees the highest responsiveness of the system to frequency changes. When in the CFV state, the notch filter zero, $z_0[n]$, is set equal to $\exp\{j2\pi\hat{f}_i[n]\}$ and $y[n]$ is filtered using (9).

D. Example of Operation

The behaviour of the multi-state notch filter is illustrated in Fig. 4 where the signal broadcast by a cigarette lighter jammer has been considered. The signal has been collected using the experimental setup described in [1]. The jamming signal spans a frequency interval of about 12 MHz in about 9 μs. The signal has been collected using a National Instruments (NI) vector signal analyzer (NI PXI-5663) with a sampling frequency $f_s = 10$ MHz. Thus the jamming signal periodically exits the front-end band. Moreover, periodic resets occur approximately each 9 μs. The time-frequency evolution of the jamming signal is shown in the upper part of Fig. 4 along with its instantaneous frequency estimated using (23) (red dashed line). The continuous black line in the upper part of Fig. 4 represents the instantaneous frequency estimated by the multi-state notch filter. It coincides with the frequency estimated using (23) only when the jamming signal is detected and considered in the CFV state. When the signal is declared out-of-band, the black curve is not plotted.

In the bottom part of Fig. 4, the different metrics used to drive the multi-state notch filter are shown. The metrics have been normalized with respect to their maximum value in order to allow their representation on a single figure. The PANOVA decision statistics, $P[n]$, combined with the decision taken on the signal presence is able to effectively determine the occurrence of a reset as clearly indicated by the spikes depicted in Fig. 4.

V. Performance Evaluation

The data collected using the experimental setup described in [1] have been used to evaluate the performance of the mult-state notch filter. The analysis involves GPS and Galileo signals generated by a Spirent GSS8000 simulator and a jamming component the power of which has been progressively increased using a variable-gain attenuator. Performance has been analyzed as a function of the Jammer-to-Noise density power ratio (J/N_0) defined as the ratio between the jamming signal power and the noise Power Spectral Density (PSD). More details about the experimental setup and the data collected can be found in [1].

The average Carrier-to-Noise density power ratio (C/N_0) loss experienced by GPS and Galileo software receivers in the presence of a jamming signals are analyzed in Fig. 5. In the figure, both the adaptive notch filter considered in [1] and the multi-state notch filter detailed above are analyzed. The adaptive notch filter considered in [1] is denoted here as 'standard'. The analysis shown in Fig. 5 has been conducted considering two contraction factors, $k_a = 0.8$ and $k_a = 0.9$, respectively.

It is possible to note that the proposed technique introduces a small loss for J/N_0 lower than 72 dB-Hz. This is due to the energy detector implemented in the filter which uses a small analysis window ($L = 5$) and a probability of false alarm, $P_{fa} = 0.01$. This implies that even in the absence of jamming, in average, 1% of the samples are declared corrupted by interference. This fact implies a small C/N_0 loss even for very low J/N_0 values. Moreover, for a J/N_0 lower than 72 dB-Hz, Prony's frequency estimator can be unreliable worsening the overall performance of the system. This loss can be avoided by introducing an additional test which declares the presence of a jamming signal considering a large number of samples. The notch filter is activated only if this preliminary test is passed. This strategy has been implemented in [1] for the activation of the standard notch filter.

The multi-state notch filter is particularly effective for high J/N_0 and outperforms the standard adaptive notch filters for J/N_0 values greater than 75 dB-Hz. For very high J/N_0 values (around 85 dB-Hz) this improvement is about 2 dB.

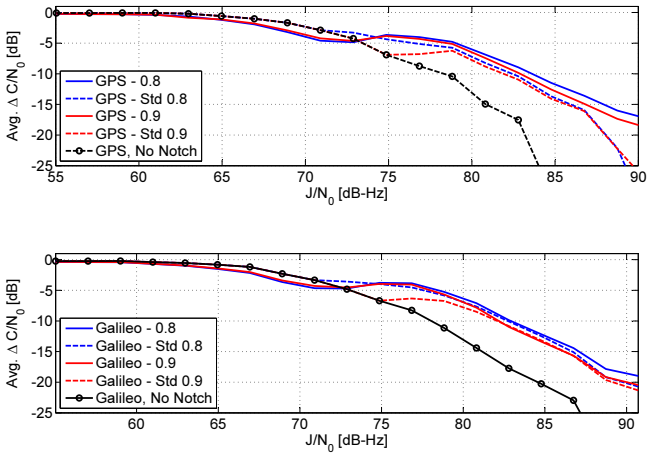

Fig. 5. Average C/N_0 losses experienced by GPS and Galileo software receivers in the presence of a jamming signal and using the adaptive notch filter considered in [1] (denoted as 'Standard - Std') and the multi-state notch filter proposed.

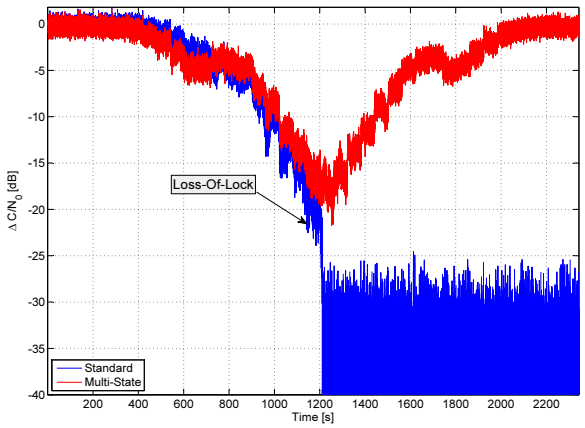

Fig. 6. C/N_0 loss experienced by a GPS software receiver when using the adaptive notch filter considered in [1] ('Standard') and the multi-state notch filter proposed. When the standard notch filter is used, the GPS receiver loses lock and thus is unable to operate for high J/N_0 values. $k_a = 0.8$.

This fact is confirmed in Fig. 6 which shows the C/N_0 loss experienced by a GPS software receiver as a function of time. The J/N_0 was increased for half of the duration of the experiment and decreased again: when the standard notch filter is used, the GPS receiver loses lock for high J/N_0 values. The multi-state approach is more effective and further improves the performance of the victim GPS receiver.

VI. Conclusions

In this paper, the signal broadcast by a GNSS jammer is analyzed from a functional point of view. In particular, it is shown that GNSS jammers broadcast single component signals which can be described using a multi-state model. The jamming signal can exit the input band of a GNSS receiver and its instantaneous frequency can be affected by abrupt changes. These effects are accounted for and a mult-state adaptive notch filter is proposed. The multi-state notch filter consists of a frequency estimator used to track fast frequency variations, an energy detector which verifies that the jamming signal is inside the receiver band and a reset detector adopted to cope with abrupt changes in the instantaneous frequency of the jamming signal.

The notch filter proposed is an effective jamming mitigation technique which is designed to be particularly effective in the presence of strong interfering signals. Experimental results show the advantages of the technique proposed with respect to adaptive notch filters previously considered in the literature.

Acknowledgments

This work has been partially supported by the European Commission in the framework of the EPCIP 2011 project (C.8325-2010 - AWP CIPS 2011).

References

[1] D. Borio, C. O'Driscoll, and J. Fortuny, "GNSS jammers: Effects and countermeasures," in *Proc. of the 6th ESA Workshop on Satellite Navigation Technologies and European Workshop on GNSS Signals and Signal Processing*, Dec. 2012, pp. 1–7.

[2] R. H. Mitch, M. L. Psiaki, S. P. Powell, and B. W. O'Hanlon, "Signal acquisition and tracking of chirp-style GPS jammers," in *Proc. of the 26th International Technical Meeting of The Satellite Division of the Institute of Navigation (ION GNSS+)*, Nashville, TN, Sep. 2013, pp. 2893 – 2909.

[3] R. H. Mitch, R. C. Dougherty, M. L. Psiaki, S. P. Powell, B. W. O'Hanlon, J. A. Bhatti, and T. E. Humphreys, "Signal characteristics of civil GPS jammers," in *Proc. of the 24th International Technical Meeting of The Satellite Division of the Institute of Navigation (ION/GNSS)*, Portland, OR, Sep. 2011, pp. 1907–1919.

[4] D. Borio, J. Fortuny-Guasch, and C. ODriscoll, "Spectral and spatial characterization of GNSS jammers," in *Proc. of the 7th GNSS Vulnerabilities Conference*. Baska, Croatia: Royal Institute of Navigation (RIN), Apr. 2013, pp. 1–17.

[5] A. Nehorai, "A minimal parameter adaptive notch filter with constrained poles and zeros," *IEEE Trans. Acoust., Speech, Signal Process.*, vol. 33, no. 4, pp. 983–996, Aug. 1985.

[6] D. Borio, L. Camoriano, and P. Mulassano, "Analysis of the one-pole notch filter for interference mitigation: Wiener solution and loss estimations," in *Proc. of the 19th International Technical Meeting of the Satellite Division of The Institute of Navigation (ION GNSS)*, Fort Worth, TX, Sep. 2006, pp. 1849–1860.

[7] L. Cohen, *Time Frequency Analysis: Theory and Applications*, 1st ed. Prentice Hall, Dec. 1994.

[8] A. Kayhan, "Difference equation representation of chirp signals and instantaneous frequency/amplitude estimation," *IEEE Trans. Signal Process.*, vol. 44, no. 12, pp. 2948–2958, Dec. 1996.

[9] T. Kraus, R. Bauernfeind, and B. Eissfeller, "Survey of in-car jammers - analysis and modeling of the RF signals and IF samples (suitable for active signal cancelation)," in *Proc. of the 24th International Technical Meeting of The Satellite Division of the Institute of Navigation ION/GNSS*, Portland, OR, Sep. 2011, pp. 430–435.

[10] B. Porat, *Digital Processing of Random Signals: Theory and Methods*. Dover Publications, 2008.

[11] S. Kay, *Fundamentals of Statistical Signal Processing, Volume II: Detection Theory*. Prentice Hall, Feb. 1998, vol. 2.

[12] D. Borio, "PANOVA tests and their application to GNSS spoofing detection," *IEEE Trans. Aerosp. Electron. Syst.*, vol. 49, no. 1, pp. 381–394, Jan. 2013.

[13] D. Borio, L. Camoriano, and L. L. Presti, "Two-pole and multi-pole notch filters: A computationally effective solution for GNSS interference detection and mitigation," *IEEE Systems Journal*, vol. 2, no. 1, pp. 38–47, Mar. 2008.